Environmental Science Processes & Impacts

ROYAL SOCIETY OF CHEMISTRY

PAPER

View Article Online
View Journal | View Issue

Check for updates

Cite this: *Environ. Sci.: Processes Impacts*, 2021, **23**, 1220

The effect of legacy gold mining on methylmercury cycling and microbial community structure in northern freshwater lakes†

Mija Aždajić, Emmanuel Yumvihoze, Jules M. Blais and Alexandre J. Poulain *

Smelting activities at Giant Mine (Yellowknife, NWT, Canada) have resulted in high sulfate and arsenic concentrations in nearby lakes. Here we tested whether historic smelting affects current mercury (Hg) cycling in 35 freshwater lakes over a 2800 km^2 area around the former gold mine. We sampled lake water and sediment over three consecutive years (2015–2017) using a factorial sampling design that accounted for different environmental variables known to affect the net methylmercury (MeHg) levels in water. Stable Hg(II) and MeHg isotope tracers were used to quantify Hg methylation and demethylation rate constants in sediments, and 16S rRNA gene amplicon sequencing was used to characterize microbial community structure. This study reveals that the fraction of methylated total Hg (% MeHg) found in surface water is positively correlated to the sulfate gradient, while the rate at which Hg is methylated (K_m) in sediments is negatively correlated with total arsenic, and positively correlated with dissolved organic carbon, total phosphorous, and % MeHg in the water. Furthermore, 6 of the 28 lakes that had detectable demethylation rate constants (K_d) also had significantly lower DOC concentrations than lakes with non-detectable K_d. Our results also show that legacy pollution from smelting activities is affecting the structure of microbial communities in lake sediments. This study reveals the complex dynamics of Hg cycling in this northern environment, highlighting the importance of large-scale studies in which the effect of multiple pollution gradients (*e.g.* arsenic and sulfate) must be taken into consideration.

Received 23rd March 2021
Accepted 16th July 2021

DOI: 10.1039/d1em00129a

rsc.li/espi

Published on 16 July 2021. Downloaded by University of Calgary on 6/22/2022 7:32:09 PM.

Environmental significance

Studies that have investigated the effect of mining activities on mercury cycling are mostly done on a small subset of lakes that cannot fully capture the range of limnological characteristics in a landscape. Our study assessed the effect of multiple variables associated with gold mining and arsenopyrite roasting (*e.g.* sulfate and arsenic concentrations) on mercury cycling on such a diverse set of lakes. Using stable mercury isotopes to measure methylation and demethylation rate constants, our results show that the sulfate concentration is a predictor of the fraction of total mercury that is present as methylmercury in the water column (% MeHg), while the rate at which microbes methylate mercury in sediments is correlated with total arsenic, dissolved organic carbon, total phosphorous, and % MeHg in water. We also show that arsenic and sulfate concentrations are significantly correlated with changes in microbial communities of sediments, along with other environmental variables (total phosphorous, and dissolved organic matter composition). Our results highlight the complex interaction between signature variables of mining activities and mercury transformations in heterogeneous landscapes.

Introduction

Mercury (Hg) is a toxic trace metal whose methylated form (*i.e.* MeHg) is a primary concern due to its neurotoxicity and ability to bioaccumulate and biomagnify in higher trophic level organisms, resulting in high [MeHg] in some predatory fish. Once in the body, MeHg can easily cross the blood–brain or placenta barriers and affect either the neurological system of a person or disrupt the normal development of a fetus.[1] As a result, understanding MeHg production and degradation in the environment is vital to protecting wildlife and humans whose diet exposes them to high levels of Hg.[2]

Whereas abiotic Hg methylation in natural environments has been shown to be possible,[3,4] Hg methylation by microorganisms is the most probable pathway to produce MeHg.[5] The identification of genes (*hgcAB*) essential for microbial Hg methylation,[6] has shown that different guilds of microbes possess the genetic potential to produce MeHg.[7–9] However, sulfate reducing microbes, which use sulfate as a terminal electron acceptor, remain important Hg methylators in freshwater environments.[10]

Although [MeHg] and [total Hg] in environmental matrices can provide information on how much Hg is methylated (*e.g.* % MeHg), these values provide only a snapshot at a given moment in time and do not address the dynamic cycling of Hg. In

Department of Biology, University of Ottawa, 30 Marie-Curie, Ottawa, Ontario K1N 6N5, Canada. E-mail: apoulain@uottawa.ca

† Electronic supplementary information (ESI) available. See DOI: 10.1039/d1em00129a

This journal is © The Royal Society of Chemistry 2021

Published on 16 July 2021. Downloaded by University of Calgary on 6/22/2022 7:32:09 PM.

particular, % MeHg does not reveal how fast the reactions proceed in a given system. It is now well established that complementing % MeHg data with methylation/demethylation experiments can offer a more complete view of MeHg dynamics,[11,12] particularly to understand how perturbations to systems (*e.g.* addition of sulfate) affect the fate of Hg.

For Hg(II) to be methylated, not only must microbes capable of Hg methylation be metabolically active, but the environmental conditions must also allow for Hg to be bioavailable to microbial cells responsible for its transformation.[13,14] Variables that affect Hg methylation, either by affecting Hg bioavailability or the activity of Hg methylating microbes, include factors such as quantity and quality of dissolved organic matter (DOM), pH, sulfate concentrations, lake productivity, iron concentrations, and temperature.[5] Multiple studies have investigated the effect of various environmental variables on Hg methylation rate constants,[15–17] with some concentrating on sites contaminated with Hg.[18,19] However, no studies have investigated the production of MeHg in a vast landscape that is greatly affected by pollution (excluding Hg) resulting from smelting activity.

Canada's North has a long history of natural resource extraction that contributes significantly to its economic sustainability[20] and development.[21] In recent years, a concerted effort was made in expanding the natural extraction industry in Canada's North, possibly affecting the landscape during and after operations, both directly (*e.g.* emission of pollutants) and indirectly (*e.g.* increased nutrient loading to local waters due to population increase).[22,23]

Here we examined factors affecting MeHg concentrations in lake waters near Giant Mine; a gold mine located on the outskirts of Yellowknife and one of Canada's largest mining operations. The mine operated from 1948 to 1999, during which time it extracted gold from arsenopyrite deposits.[24] The arsenopyrite deposits found in the Yellowknife area consist of a refractory ore that is resistant to normal extraction techniques like cyanidation due to the presence of sulfides. Thus the ore was first smelted to release sulfur, followed by cyanidation to collect the gold.[25] The smelting of metal ores released great quantities of pollutants into the atmosphere that were later deposited on the surrounding landscape, making this area one the most polluted sites in Canada.[26] Many studies in the last decade have shown the extent of pollution far beyond the Giant Mine lease boundaries.[27–30] In particular, Houben *et al.* (2016) showed that arsenic (2.0–136 $\mu g\ L^{-1}$), antimony (0.1–2.0 $\mu g\ L^{-1}$), and sulfate (0.5–48 $mg\ L^{-1}$) concentrations in lake water decreased with distance from the roaster stack. These anthropogenic stressors can potentially affect the biogeochemical cycling of metals in the environment, particularly Hg.

Smelting operations have resulted in a 'halo' of high [sulfate] (up to 115 $mg\ L^{-1}$) in lakes near Giant Mine (<25 km). Although [total Hg] in the lakes remain within concentrations typical of these sub-Arctic environments (1–6 $ng\ L^{-1}$),[31] the ratio of MeHg relative to total Hg (% MeHg) is higher close to the mine and decreases with distance.[27] These aquatic systems presented a great opportunity to study the effect of sulfate loading on Hg methylation in northern freshwater lakes. We hypothesized that enhanced sulfate deposition from smelting affected MeHg dynamics in sediments of lakes surrounding Giant Mine. Assuming that sulfate reducing metabolism was the main variable limiting [MeHg] in the system and not the amount or delivery rate of bioavailable mercury, we predicted that [sulfate] would be positively correlated with both rates of MeHg production and % MeHg.

We tested our hypothesis by (i) identifying which chemical variables correlated with MeHg production in lakes around Giant Mine, and (ii) quantifying Hg methylation/demethylation rate potentials in lake sediments along the sulfate gradient around Giant Mine using stable isotopes of Hg. We also measured environmental variables that likely influence microbial Hg cycling. To further assess the response of the microbial community, we characterized changes in microbial community structure along the pollution gradient. We used these changes as one integrative response to the geochemical variation present across the spatial gradient sampled.

Materials and methods

Study sites

Sampling took place within a 30 km radius around the Giant Mine roaster stack (Fig. 1). This radius of sampling was chosen to include reference sites unaffected by the mining activity based on studies that have shown the full extent of the roasting emissions being within a 25 km radius.[27] Lakes in the Yellowknife area were sampled during three years (2015, 2016, and 2017) using a factorial sampling design while attempting to account for variables that may be important in directly or indirectly affecting [MeHg] in freshwater ecosystems such as aqueous [sulfate], [DOC], [total iron], [total phosphorus], and pH. Fig. 2, a principal component analysis (PCA) of the water chemical variables, shows an orthogonal distribution of the concentration gradients for the environmental variables mentioned above.

Both surface lake water and the top 5 cm of sediment were sampled at each lake. The sampled surface water was acidified and stored at 4 °C. Sediment was sampled in triplicate using a Uwitec corer. The top 5 cm of each core was subsampled, using an extruder, into a sterile bag and a small amount of sediment was put into cryotubes using a sterile spatula. The cryotubes were flash-frozen with dry ice and preserved at −80 °C until further analyses. Due to logistical constrains, the rest of the sediment was frozen and preserved at −20 °C until analysis.

Water chemistry

Triplicate surface water samples were analysed for total Hg as described in EPA method 1631 using cold-vapor atomic fluorescence spectrometry (CV-AFS, Tekran Instrument Corp. Series 2600 spectrophotometer)[32] (average recovery of laboratory control sample: 97.66%). MeHg in water was extracted using the method described in Cai *et al.* (1997) and analysed with capillary gas chromatography-atomic fluorescence spectrometry (GC-AFS, Ai Cambridge Model 94 GC with a CTC Autosampler and PSA Merlin Detector)[33] (average recovery of laboratory control sample: 88.51%).

Total arsenic and total phosphorous concentrations were measured by inductively coupled plasma mass spectrometry

Published on 16 July 2021. Downloaded by University of Calgary on 6/22/2022 7:32:09 PM.

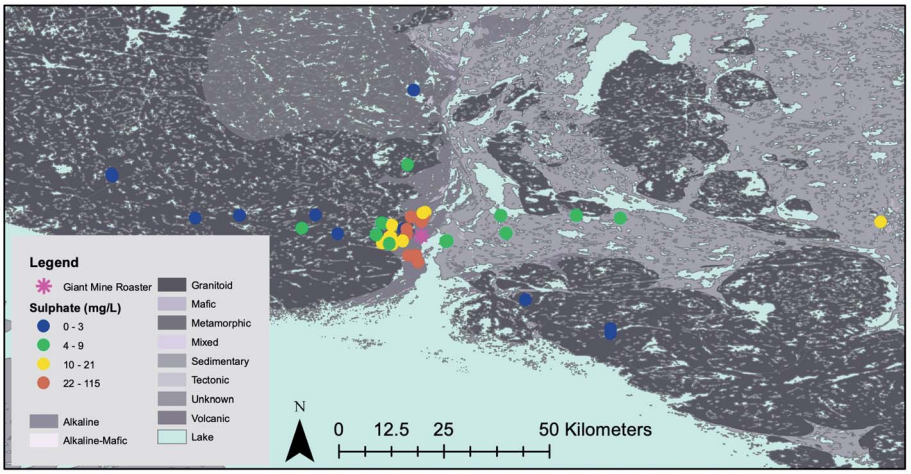

Fig. 1 Map of sampling sites in Yellowknife, NWT, Canada. Each point represents a lake sampled during the study in 2015, 2016, and 2017.

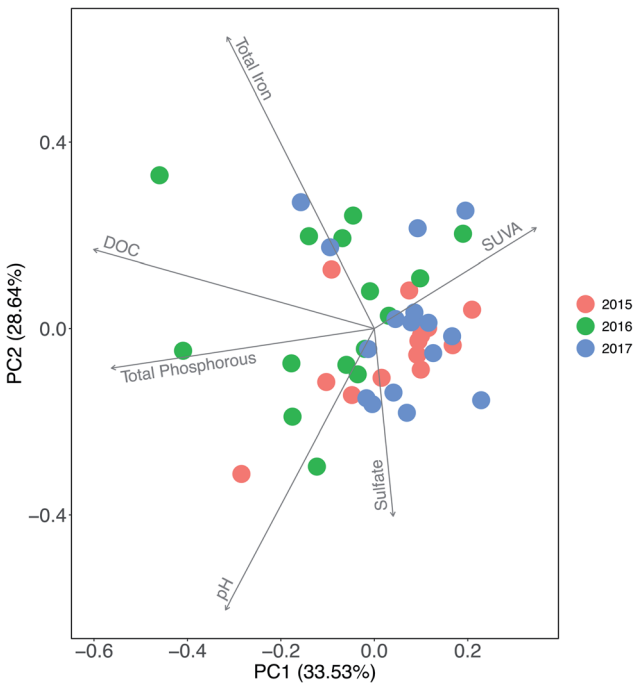

Fig. 2 A principal coordinate analysis (PCA) plot showing the differences in water chemistry of each lakes sampled. Points represent the sampled lakes and the arrows of water chemistry for each lake during the three year.

(ICP-MS) using EPA method 200.8 (ref. 34) (average recovery of laboratory control sample: 102.30%).

$SUVA_{254}$ (L mg^{-1} m^{-1}) is the ratio of absorbance at UV254 and [DOC] in the water, this ratio can be used as a general quantitative estimate of aromaticity of DOC in the sample.[35] The absorbance UV_{254} was measured with a spectrophotometer (Cary 300 BIO UV-vis Spectrophotometer) and [DOC] were measured using a modified OI Analytical model 1030 wet TOC analyser, with a model 1051 autosampler.[36]

All other chemical analyses (*i.e.* total iron, pH, sulfate, and total nitrogen) with water samples were done at Taiga Environmental Laboratory (Yellowknife, NWT, Canada), which is certified by the Canadian Association for Laboratory Accreditation (CALA) (ISO/IEC 17025).

Incubation experiments

The lake sediments were thawed overnight at 4 °C. In each vial, 18 g of homogenized sediment was mixed with 54 mL of anaerobic milliQ (1 : 3 slurry ratio) in the anaerobic chamber. The slurry was prepared in a serum vial with a rubber stopper to ensure no oxygen would penetrate into the slurry samples. The slurry was first left at 4 °C for 3 days, then overnight at room temperature in the anaerobic chamber.

Two treatments, each in triplicate, were applied to each lake sediment sample. The first treatment was spiked with $Me^{198}Hg$ and ^{199}Hg solutions (prepared in milliQ and left to equilibrate for 2 hours in a cool dark space), the second was left unspiked to track the natural variation in isotope concentrations. The spiked treatments had a final concentration of 10 ng g^{-1} of ^{199}Hg (inorganic) and 5 ng g^{-1} of $Me^{198}Hg$, respectively representing on average 114% and 278% of the Hg and MeHg already present in the system. 2.5 g of sediment were subsampled at each time point (0 h, 6 h, 12 h, 24 h, 48 h) and flash frozen in liquid nitrogen. Samples were stored at −20 °C, then freeze-dried and stored in a cool dark place until analysis.

Several MeHg extraction methods were tested due the large number of lakes with different chemical and geological properties. Ultimately, a modified Cai *et al.* (1997)[37] extraction method was found to yield the best results, as demonstrated by an average 92.50% recovery rate of $Me^{198}Hg$ isotope. Freeze-dried samples were weighted out and placed into a glass vial, 5 mL of 4 M nitric acid (HNO_3) were added. An internal isotope standard ($Me^{201}Hg$) was added and samples were left in a dark cool place for 30 minutes. Following this, samples were placed in an oven at 55 °C for 16 hours. After, 0.5 mL of 1.0 M copper sulfate ($CuSO_4$) was added to cooled samples along with 7 mL of dichloromethane (DCM). The mixture was shaken for 3 hours, then centrifuged for 10 minutes at 3500 rpm. The overlying DCM was then extracted

 This journal is © The Royal Society of Chemistry 2021

Published on 16 July 2021. Downloaded by University of Calgary on 6/22/2022 7:32:09 PM.

into a second glass vial and 2 mL of 1 mM sodium thiosulfate solution ($Na_2S_2O_3$) was added. The mixture was then shaken for 1 hour and centrifuged for 10 minutes at 3500 rpm. Finally, the overlying sodium thiosulfate was removed and placed into an amber GC vial for analysis. Hg isotopes were then analyzed using liquid chromatography inductively coupled plasma mass spectrometry (LC-ICP-MS) following the method described in Batista *et al.* (2011)[38] (Table S1 and Fig. S4†).

First, for each lake, a linear segment of the methylation and demethylation figure (Fig. S4†) was visually assessed to find the best time point for maximum methylation/demethylation rates. Next, a pseudo first-order relationship for mercury species was assumed, and both the first-order methylation rate constant (K_m, eqn (1)) and the first-order demethylation rate constant (K_d, eqn (2)) were calculated based on Hintelmann *et al.* (2000).[39–41] Considering that the Hg isotopes that are added to sediments have been shown to be more bioavailable that ambient Hg,[41] the calculations henceforth will refer to the potential methylation/demethylation rate constants of each lake sediment. Most of the lakes for which we determined K_d (22 out of 28) did not show clear demethylation, with K_d values either around zero or even slightly positive (Fig. S4†). We did not setup "killed" experiments for every lake sediment types to obtain control K_d values; this was not logistically possible considering our field constraints. In absence of this dataset and to provide an estimate of the variance associated with K_d, we used 3 times the standard deviations around the average K_d for lakes that did not show demethylation; we used this value as our limit of quantification (LOQ = 0.304 d^{-1}) to include lakes in our statistical analyses. Note that raw data are provided in ESI.†

$$K_m = \frac{\left[Me^{199}Hg\right]_{t24} - \left[Me^{199}Hg\right]_{t0}}{\left[^{199}Hg\right]_{spiked} \times t} \quad (1)$$

$$K_d = -1 \times \frac{\ln\left[Me^{198}Hg\right]_{t24} - \ln\left[Me^{198}Hg\right]_{t0}}{t} \quad (2)$$

Microbial community structure

Sediment DNA was extracted using the MoBio PowerSoil DNA Extraction Kit following the manufacturer's instructions. The quality of DNA extracted was tested ensuring that PCR targeting 16S rRNA and *gln*A genes yielded amplicons of the correct size visible by gel electrophoresis. 16S rRNA gene amplicons were sequenced using Illumina MiSeq with primers 341F (CCTACGGGNGGCWGCAG) and 785R (GACTACHVGGGTATCTAATCC) targeting the V3–V4 region at the MR DNA sequencing facility (Shallowater, Texas, USA).

16S rRNA gene amplicon sequencing results were analyzed with a QIIME2 pipeline using DADA2 (ref. 42) to infer amplicon sequences and the SILVA 138 database to assign taxonomy.[43] All statistical analyses found in this study pertaining to the microbial community of the lakes were done in R with the following packages: phyloseq,[44] vegan,[45] and ggvegan.[46] The details pertaining to the pipeline analysis can be found in a github repository (mijaazdajic/ykn_QIIME_analysis).

Statistical analyses

Three main statistical techniques were used to analyze the results: general linear regression analyses, unconstrained ordinations, and constrained ordinations. All statistical analyses were done in R with the following packages: vegan[45], MASS[47], lmtest,[48] and car.[49] The full analyses can be found in a github repository (mijaazdajic/ykn_R_statistical_analyses).

To analyze which environmental variable best correlated with % MeHg and Hg kinetics (K_m and K_d), we used a stepwise regression analysis to build the best regression model. All residuals of models were tested for model assumptions (*i.e.* linearity, homoscedasticity, and normality).

An unconstrained multivariate ordination was used to assess the differences in chemical composition of water samples. Each sampling site had four different environmental variables (*i.e.* sulfate, pH, DOC, total iron) that were normalized and used to make a Euclidean distance matrix. Then, this distance matrix was used in a PCA.

Spatial distances between sampling sites were transformed into rectangular vectors by principal coordinates of neighbour matrices (PCNM).[50] This transformation reflects the spatial relationships among sampling sites using vectored variables, which are then directly included as covariates in constrained ordinations, allowing to test if the geographic placement of sites explained the changes in microbial community composition.

A UniFrac dissimilarity matrix was calculated to assess the differences in microbial community structures of the sampled lake sediments. UniFrac metrics rely on the phylogenetic distances of microbial communities between samples. Here, we report on the weighted UniFrac metric which considers both phylogenetic relationship and differences in abundance between sampling sites. Using the Unifrac distance matrix, we performed distance based redundancy analysis (db-RDA) to test variability of microbial communities against spatial, environmental, and kinetic (K_m/K_d) data. A db-RDA analysis implements classical multidimensional scaling on a dissimilarity matrix and performs a redundancy analysis on the ordination results to measure the variation explained by a given set of explanatory variables. A db-RDA was chosen because (i) it is a constrained analysis complementary to a principal coordinate analysis (PCoA), therefore appropriate to use with non-Euclidean distance matrices such as UniFrac, (ii) it has been shown to be more powerful than the commonly used Mantel correlation test,[51] and (iii) it does not assume multi-normality in the response variables.[52] We performed a stepwise model selection in order to minimize the number of variables in the analyses and used ANOVA-like permutation tests to assess the significance of coefficients. All analyses were handled with the *vegan* package in R.[45]

Results and discussion

Giant Mine smelting operations created a gradient of sulfate (0–115 mg L^{-1}) in a wide area for which the levels of Hg in lakes remain within natural concentrations (1–6 ng L^{-1}).[31] Based on our current knowledge of MeHg production, we predicted that increasing [sulfate] would stimulate sulfate-reducing microbial

Published on 16 July 2021. Downloaded by University of Calgary on 6/22/2022 7:32:09 PM.

metabolism which would result in more MeHg (% MeHg) and higher rate of MeHg production (K_m).

We first set out to choose lakes that were broadly representative of the geochemistry of the region surrounding Giant Mine by sampling lakes in a large geographic area (Fig. 1 and Table 1), which we sampled over three years (2015–2017). This spatial variability allowed us to capture the effect of multiple environmental variables on MeHg cycling namely in terms of pH, [sulfate], [DOC], [total phosphorous], and [iron], which are important variables known to affect MeHg production[5] (Fig. 2). We also explored the role of arsenic, a toxic metalloid, that could possibly confound the results due to the strong gradient that is present in the lakes studied (0.42–1327 μg L^{-1}).

Our first objective was to identify which environmental variables (sulfate, arsenic, iron, DOC, pH, phosphorous) were correlated with % MeHg observed in lakes. Using a step-wise regression model, [sulfate] in water was the only environmental variable that was significantly correlated with % MeHg in the water column (p-value < 0.05). The relationship between % MeHg and [sulfate] was nonlinear ($\log(y) = \log(x) + a$) and reached a plateau at *ca.* [sulfate] = 40 mg L^{-1} (Fig. 3a). Most studies show significant non-linear relationships between [sulfate] and [MeHg][53,54] or methylation rate constants,[17] and most systems do reach a level at which addition of sulfate does not stimulate production of MeHg.[11,55] This phenomenon is mostly attributed to the relationship between Hg and sulfide, a by-product of sulfate reduction. At low [sulfate], the additions of sulfate stimulate sulfate-reducing microbial metabolism, leading to an increase in the production of MeHg.[10] As sulfide concentrations increase, mercury sulfide complexes form aggregates that are less bioavailable. Therefore, less Hg is methylated in the system due to decreased bioavailability to Hg methylating microbes.[56,57]

However, the bioavailability of Hg species is not the only variable that can affect the final concentrations of MeHg in the surface water. Limnologic characteristics, such as lake and catchment size, have been shown to affect the concentrations of total Hg and MeHg in water.[58] The relationship between the production (K_m) and degradation (K_d) of MeHg in the system is also important to consider. Net [MeHg] (and % MeHg) is the result of both MeHg production and MeHg degradation;[59] hence identifying the environmental variables that affect the rate of

Table 1 Information of lakes sampled including sampling spatial coordinates, aqueous Hg and MeHg concentrations, and Hg transformation rate constants. (LOQ = limit of quantification)

Lake	Latitude	Longitude	Area (m^2)	MeHg (ng L^{-1})	THg (ng L^{-1})	K_m (d^{-1})	K_d (d^{-1})
BC14	62° 31′ 30.57″ N	114° 25′ 07.48″ W	193 952	0.79	2.92		
BC17	62° 29′ 59.45″ N	114° 25′ 14.90″ W	156 331	0.29	1.97	0.194	<LOQ
BC18	62° 31′ 04.57″ N	114° 23′ 40.92″ W	155 789	0.15	1.41	0.038	<LOQ
BC20	62° 30′ 19.50″ N	114° 23′ 16.03″ W	437 109	1.15	2.32	0.263	<LOQ
BC21	62° 29′ 16.61″ N	114° 26′ 23.85″ W	92 916	0.07	0.96	0.085	<LOQ
BC22	62° 32′ 27.31″ N	114° 50′ 24.64″ W	8301	0.28	1.63		
BC24	62° 32′ 48.05″ N	114° 44′ 43.27″ W	11 384	0.08	0.99	0.013	<LOQ
BC30	62° 31′ 08.11″ N	114° 36′ 43.51″ W	622 416	0.04	0.33	0.167	<LOQ
BC31	62° 32′ 50.16″ N	114° 34′ 57.98″ W	349 068	0.09	1.35		
BC32	62° 30′ 26.04″ N	114° 32′ 07.44″ W	118 138	0.30	1.26		
BC36	62° 32′ 27.12″ N	113° 55′ 51.05″ W	132 511	0.37	5.80	0.137	<LOQ
BC43	62° 30′ 30.65″ N	114° 10′ 30.04″ W	358 987	0.09	0.55	0.147	<LOQ
BCR07	62° 32′ 34.62″ N	114° 21′ 09.83″ W	14 069	0.21	0.93	0.237	<LOQ
David	62° 32′ 36.46″ N	114° 22′ 37.31″ W	132 815	0.15	0.69	0.084	<LOQ
Frame	62° 27′ 38.19″ N	114° 23′ 02.53″ W	881 244	0.18	0.70	0.021	0.483
Icing	62° 39′ 18.75″ N	114° 23′ 08.23″ W	1 210 000	0.10	0.77	0.010	1.166
Martin	62° 31′ 49.49″ N	114° 26′ 26.49″ W	2 929 991	0.13	0.42		
BCR-Mija	62° 31′ 55.45″ N	114° 21′ 21.62″ W	15 016	0.18	0.80	0.398	<LOQ
Niven	62° 27′ 41.36″ N	114° 22′ 04.52″ W	107 463	0.98	2.19	0.743	<LOQ
Pocket	62° 30′ 32.30″ N	114° 22′ 25.60″ W	48 000	0.75	2.50		
Pontoon	62° 32′ 46.31″ N	114° 01′ 28.79″ W	3 534 190	0.07	0.26	0.313	<LOQ
Prosperous	62° 32′ 47.92″ N	114° 11′ 10.84″ W	160 930 000	0.02	0.22	0.073	0.318
Rat	62° 26′ 45.22″ N	114° 21′ 48.95″ W	38 213	0.60	1.08	0.192	<LOQ
Vee	62° 33′ 04.01″ N	114° 21′ 12.94″ W	697 807	0.22	0.52		
YK11	62° 29′ 05.43″ N	114° 25′ 03.53″ W	548 597	0.27	0.71	0.088	<LOQ
YK12	62° 29′ 09.19″ N	114° 25′ 30.33″ W	64 225	0.30	3.03	0.325	<LOQ
YK40	62° 21′ 59.63″ N	114° 08′ 01.50″ W	340 232	0.05	0.74	0.170	<LOQ
YK42	62° 29′ 31.57″ N	114° 23′ 46.52″ W	212 361	0.14	0.95	0.058	0.522
YK60	62° 30′ 18.15″ N	114° 27′ 11.94″ W	393 444	0.03	0.28	0.013	0.972
YK67	62° 29′ 31.24″ N	114° 18′ 06.58″ W	87 674	0.10	2.16	0.068	<LOQ
YKE1	62° 31′ 54.77″ N	113° 22′ 23.76″ W	227 031	0.10	0.52	0.083	<LOQ
YKN1	62° 48′ 48.50″ N	114° 22′ 13.95″ W	260 633	0.04	0.41	0.086	<LOQ
YKS1	62° 17′ 37.92″ N	113° 57′ 06.36″ W	202 589	0.12	0.65	0.171	0.432
YKS2	62° 18′ 14.64″ N	113° 57′ 04.74″ W	2 347 017	0.02	0.32	0.156	<LOQ
YKW1	62° 38′ 06.87″ N	115° 01′ 08.62″ W	928 750	0.13	0.93	0.250	<LOQ

 This journal is © The Royal Society of Chemistry 2021

Published on 16 July 2021. Downloaded by University of Calgary on 6/22/2022 7:32:09 PM.

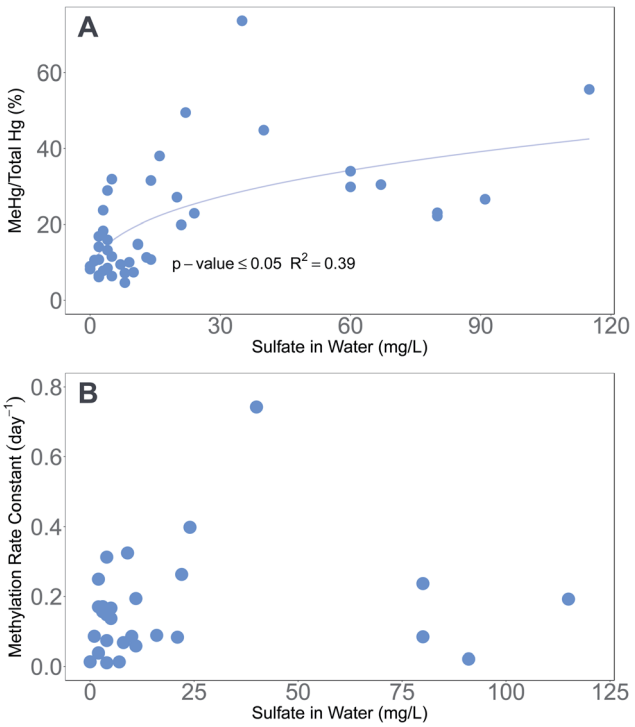

Fig. 3 Results from chemical and incubation experiments. Panel A shows % MeHg with respect to sulfate concentrations in the water column of all lakes from the study. Panel B shows the methylation rate constant (d^{-1}) in the sediments with respect to sulfate concentration in the water column.

MeHg transformations will help better identify how emissions from Giant Mine affected the final % MeHg in the systems.

The potential rate constants of Hg methylation in our study ranged from 0.010 d^{-1} to 0.743 d^{-1} with an average of 0.163 d^{-1}, which is comparable to rate constants found in other lake sediments[40,60,61] wetland systems.[11,17,62–65] We used stepwise regression to identify which of the environmental variables collected in the water column (sulfate, arsenic, pH, DOC, SUVA, total iron, total phosphorus, and % MeHg) best explained changes in K_m in the studied lakes sediments. Our statistical analysis (Table 2 and Fig. S1†) revealed that four environmental variables were significantly correlated with K_m; total arsenic (p-value = 0.0129), DOC (p-value = 0.0467), total phosphorous (p-value = 0.0301), and % MeHg (p-value = 0.0039).

Total arsenic concentration was negatively correlated with K_m. The literature seldom refers to the interplay between arsenic and Hg, and we could not find any studies that addressed this possible relationship over large spatial scales. Our results show that the historical arsenic pollution gradient does have an effect on the production of MeHg in lakes around Giant Mine, possibly limiting methylation due to the toxic nature of arsenic.[66,67]

DOC had a positive and significant relationship with K_m. The role of dissolved organic matter (DOM), for which we measured [DOC] as a proxy, is complex. DOM can affect Hg bioavailability, both increasing and decreasing it.[60,68–70] First, DOM can help stabilize Hg–sulfide complexes[71,72] and can increase the bioavailability of these complexes to Hg methylating microbes,[73] however aged DOM can decrease the bioavailability of Hg.[68] Secondly, DOC can also stimulate microbial metabolism acting as carbon and energy sources.[69,74] Additionally, studies have shown that the origin (*i.e.* composition) of the DOM can affect the final production of MeHg in freshwater systems.[60] In fact, SUVA was also identified during the model selection; however, in the selected model, the relationship between SUVA and K_m fell marginally short of significance (p-value = 0.088).

Table 2 Results from the step-wise regression model selection. Regression model (R^2 = 0.329, $F(5, 22)$ = 3.653, p-value = 0.0148) below was chosen to best explain the changes in Hg methylation rate constants (K_m) in sediments

Variable	Estimate	St. dev	T	p-Value
(Intercept)	−7.1855	1.3081	−5.493	<0.0001**
ln(SUVA)	0.7195	0.4030	1.785	0.0880
ln(Total arsenic)	−0.2915	0.1077	−2.706	0.0129*
ln(DOC)	0.7049	0.3344	2.108	0.0467.
ln(Phosphorous + 1)	0.4263	0.1839	2.318	0.0301*
ln(% MeHg)	0.9230	0.2862	3.225	0.0039**

Total phosphorous, which we used as a proxy for lake productivity,[75,76] was also positively and significantly correlated with K_m. It is reasonable to expect methylation rate constants to increase with increasing productivity of the lakes, as shown by other studies, possibly providing labile carbon sources to microbes.[16,77]

Finally, our analysis revealed that % MeHg in water was positively correlated with K_m measured in sediments, which is in agreement with other studies.[12,62] Indeed, MeHg that is produced in the sediments is one of the largest contributors of MeHg in the water column.[40]

Although sulfate was significantly correlated with % MeHg, our analysis did not show sulfate in water as being a significant predictor of K_m in sediments (Fig. 3b). This is not unexpected as sulfate levels in water do not necessarily reflect sediment porewater sulfate levels, due to the rapid cycling of sulfate in lacustrine sediments.[78] However, examination of the relationship between K_m and [sulfate] (Fig. 3b) clearly shows that four lakes with the highest sulfate concentrations clustered together, possibly standing as outliers. These lakes all have [sulfate] > 40 mg L^{-1}, which is also the threshold above which we observed a plateau in the relationship between % MeHg and [sulfate] (Fig. 3a). We decided to run an analysis without these four lakes on the basis of their high [sulfate], above the threshold at which evidence suggested methylation is hampered (here, *ca.* 40 mg.L^{-1}). Two regression models were found to best explain the changes in K_m in sediments (Fig. S2†). The first regression model identified sulfate as significantly and positively correlated with K_m (p-value = 0.03, R^2 = 0.15), while the second regression model identified % MeHg as being significantly and positively correlated with K_m (p-value = 0.04, R^2 = 0.15). Considering that the Akaike information criterions (AIC) for both regression models were very similar (71.74 and 71.95 respectively) and that there was no statistically significant difference between the two models (p-value > 0.05), we conclude

Published on 16 July 2021. Downloaded by University of Calgary on 6/22/2022 7:32:09 PM.

that both variables are equally good predictors of K_m in the system. Therefore, for this subset of lakes (with only 4 lakes with very high [SO_4^{2-}] that were excluded), we can infer that K_m is significantly correlated to the pollution gradient (*i.e.* [sulfate] in the water column) as well as % MeHg in the water column. This suggests that the activity of Hg methylators (*e.g.*, sulfate reducers) is likely affected by the pollution gradient and that this effect could result in the gradient of % MeHg we have observed. However, it should be highlighted that 4/28 lakes (*ca.*15% of samples) were not included in this subset of lakes, suggesting that this predictive model may only be applicable to lakes with [sulfate] $\leq$ 40 mg.L^{-1}, a threshold above which additional variables are needed to explain $K_m = f$([sulfate]).

Mercury methylation is a microbially mediated process. We used 16S rRNA gene amplicon sequencing as a means to test whether the pollution gradient affected the microbial community structure, and explored how these changes might be associated with variations in MeHg transformation rate constants.

Variables that could possibly be related to microbial community structure were divided into three categories: spatial variation (spatial relationships among sampling sites using vectored variables, PCNM), water chemistry (*i.e.* [DOC], pH, [sulfate], [total Fe], [total phosphorous], [total arsenic], and SUVA), and Hg transformation rate constants (*i.e.*, K_m and K_d). Following a stepwise regression, our results indicated that two of the major pollutants emitted from Giant Mine smelting, namely sulfate (p-value 0.004) and arsenic (p-value = 0.001), were significantly correlated with changes in microbial community structure together with total phosphorous (p-value = 0.045) and SUVA (p-value = 0.040). The constrained ordination (db-RDA) showed that 28.42% of the total variation of microbial community structure was explained by these variables with each axis explaining 42.67%, 28.75%, 16.98%, and 11.60% of the fitted variation. Using a partial db-RDA analysis we showed that 10.50% of variation could be attributed to [total arsenic], 6.65% to [sulfate], 5.68% to SUVA, and 5.59% to [total phosphorous] (Fig. 4 and Table 3). Admittedly, the variability explained within microbial community structure can be considered small. This reflects the complex interplay of variables affecting microbial community structure in environmental samples and to the fact that we likely have not measured all possible explanatory variables.

Interestingly, the two variables that significantly correlated with K_m (Table 2) were also significantly correlated with changes in microbial community: arsenic and phosphorous concentrations. Some studies have found that arsenic can alter microbial community structure and diversity,[79] while other studies have found no significant effect.[67] Total phosphorous has also been found to influence microbial community structure[80] and phosphate has specifically been shown to increase the activity of heterotrophic microbes.[81] The correlation between arsenic and total phosphorous with both changes in microbial community structure and K_m indicate that variation in the structure of the microbial community due to changes in nutrients or toxicant concentrations possibly affect Hg methylation. When a db-RDA was performed for the subset of lakes for which incubation data was available (Table 4 and Fig. 5), only [total arsenic] was significantly correlated with changes in microbial community (p-value = 0.002) explaining 16.20% of the fitted variability. Obtaining additional information on the genetic potential of these microbial communities to methylate Hg, such as *hgc*AB genes, diversity, and abundance would allow to better constrain this variability.[6,9]

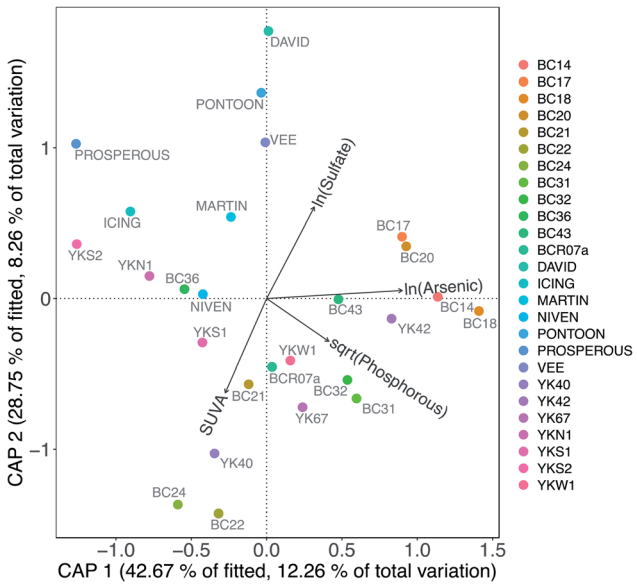

Fig. 4 Distance based redundancy analysis (db-RDA) plot of microbial community based on the chemical and spatial variables. This analysis was done on all lakes sampled during the study.

Table 3 Results from stepwise model (ordistep) for the constrained ordination method (db-RDA). This analysis was done on all lakes sampled during the study

Variable	Sum of squares	Pseudo F	p-Value
ln(Total arsenic)	0.4482	3.1209	0.001**
ln(Sulfate)	0.2954	2.0566	0.004**
sqrt(Total phospohorous)	0.2320	1.6153	0.045
SUVA	0.2405	1.6748	0.040*

Our results also indicate that DOM origin (characterized by SUVA) was a significant contributor to the microbial community structure of these northern lakes. SUVA can be used as a proxy for DOC origins, samples with high SUVA ($\geq$4 L mg^{-1} m^{-1}) tend to have more complex and heterogenous organic compounds that are rich in aromatics, while samples with lower SUVA (<3 L mg^{-1} m^{-1}) tend to have more homogenous and low-molecular weight molecules that are low in aromatics.[82] This value provides information on the source of the DOM in the water column; water samples with high SUVA indicate a large presence of allochthonous DOM in the water column, while lower values are indicative of autochthonous sources of DOM.[83] SUVA in the lakes ranged from 0.029 L mg^{-1} m^{-1} to 2.400 L mg^{-1} m^{-1}, with an average of 0.846 L mg^{-1} m^{-1} which is comparable to other northern Canadian lakes.[84] The SUVA between the lakes spans two orders of magnitude indicating that certain lakes were possibly receiving more allochthonous DOM than others, although all samples seem to indicate a larger presence of

 This journal is © The Royal Society of Chemistry 2021

Published on 16 July 2021. Downloaded by University of Calgary on 6/22/2022 7:32:09 PM.

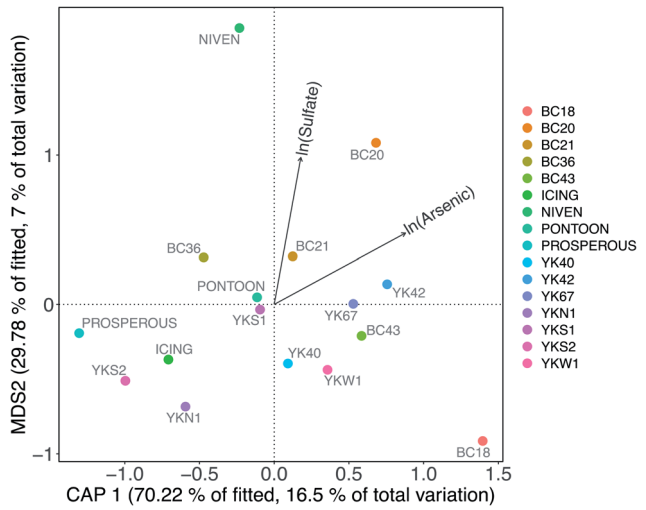

Fig. 5 Distance based redundancy analysis (db-RDA) plot of microbial community based on the chemical, spatial, and kinetic variables. This analysis was done on all lakes for which incubation data was available.

Table 4 Results from stepwise model (ordistep) for the constrained ordination method (db-RDA) for the subset of lakes for which incubation data was available

Variable	Sum of squares	Pseudo F	p-Value
ln(Total arsenic)	0.3710	2.3432	0.002*
ln(Sulfate)	0.2371	1.5571	0.050

homogenous and low-molecular weight molecules. Autochtonous organic matter has been shown to enhance methylation rates in boreal lake sediments by increasing overall microbial activity,[60] however SUVA was not identified as an significant predictor of % MeHg nor K_m in the set of lake studied here. Therefore, our results show that carbon substrate (*i.e.* DOC) availability is associated with both the assemblage of microbes in sediment and the activity of Hg methylating microbes, although only the microbial community structure seems to be significantly affected the by the nature of this carbon substrate.

MeHg demethylation rate constants (K_d) ranged between below the limit of quantification (LOQ = 0.304) to 1.166 d^{-1} which is comparable to other studies both in lakes[60,61] and wetlands.[55,62,65] Note that 22 out of 28 lakes sampled had K_d below LOQ during incubations (Fig. S4†). Considering the large number of values below LOQ in our dataset, we could not meet normality nor linearity assumptions of residuals for a general linear regression model. However, we separated the lakes into two groups: lakes for which K_d > LOQ and those for which K_d < LOQ, and tested whether environmental variables were significantly different between the two groups using a non-parametric test (Fig. S3†). DOC was the only variable that was significantly different between the two groups of lakes (p-value < 0.01) with the lakes that exhibited demethylation having significantly lower [DOC], which could be linked to decreasing bioavailability of MeHg.[85] This contrasts with studies that have shown that demethylation increases with increasing organic carbon concentrations in the system,[86] and others that have not found any significant correlation between K_d and DOC.[19,87]

To conclude, Hg cycling in lakes around Giant Mine is affected by several variables associated with historical mining activities. The fraction of total Hg found as MeHg (% MeHg) in these Yellowknife lakes is significantly correlated with the historical deposition of sulfate from Giant Mine. The rate at which MeHg is formed in the sediments (*i.e.* K_m) is negatively correlated with total arsenic, and positively correlated with DOC, total phosphorous, and % MeHg in the water. However, only a subset of lakes has a significant correlation between Hg cycling kinetics (*i.e.* K_m) and the sulfate concentration gradient in this landscape. These results speak to the complexity of Hg cycling in a heterogeneous landscape. The majority of studies that investigate Hg cycling in the environment usually concentrate on a few lakes or sampling sites, mostly along Hg pollution gradients.[12,17,19,62,63,88] This limits the environmental variables that can be controlled for, and might ultimately affect the conclusions that are drawn from these results. Our results, collected over 3 years and covering 2800 km^2 highlight the importance of conducting larger scale landscape studies in which we can investigate the effect of coincident pollution gradients (*e.g.* arsenic and sulfate) affecting Hg cycling.

Conflicts of interest

There are no conflicts to declare.

Acknowledgements

The authors would like to thank David Eickmeyer, Cynthia Cheney, Martin Pothier, Branaavan Sivarajah, Claudia Tanamal, Emily Stewart, Mike Palmer, and Jennifer Korosi for their assistance in the field and Linda Kimpe for the logistical planning of all three field seasons. This work was funded by an NSERC DG to AJP, a Strategic Grant from the Natural Science and Engineering Research Council of Canada (NSERC) (Grant # STPGP 462955-14 (to JMB, AJP, and JPS)) and the Northern Scientific Training Program (CLC).

References

1 E. M. Sunderland and M. Tumpney, in *Persistent Organic Pollutants and Toxic Metals in Foods*, ed. M. Rose and A. Fernandes, Woodhead Publishing, 2013, pp. 392–413.
2 C.-C. Lin, N. Yee and T. Barkay, in *Environmental Chemistry and Toxicology of Mercury*, John Wiley & Sons, Ltd, 2011, pp. 155–191.
3 V. Celo, D. R. S. Lean and S. L. Scott, Abiotic methylation of mercury in the aquatic environment, *Sci. Total Environ.*, 2006, **368**, 126–137.
4 J. H. Weber, Review of possible paths for abiotic methylation of mercury(II) in the aquatic environment, *Chemosphere*, 1993, **26**, 2063–2077.

Published on 16 July 2021. Downloaded by University of Calgary on 6/22/2022 7:32:09 PM.

5 A. R. Paranjape and B. D. Hall, Recent advances in the study of mercury methylation in aquatic systems, *FACETS*, 2017, **2**, 85–119.
6 J. M. Parks, A. Johs, M. Podar, R. Bridou, R. A. Hurt, S. D. Smith, S. J. Tomanicek, Y. Qian, S. D. Brown, C. C. Brandt, A. V. Palumbo, J. C. Smith, J. D. Wall, D. A. Elias and L. Liang, The Genetic Basis for Bacterial Mercury Methylation, *Science*, 2013, **339**, 1332–1335.
7 G. A. Christensen, A. M. Wymore, A. J. King, M. Podar, R. A. Hurt, E. U. Santillan, A. Soren, C. C. Brandt, S. D. Brown, A. V. Palumbo, J. D. Wall, C. C. Gilmour, D. A. Elias and G. Voordouw, Development and Validation of Broad-Range Qualitative and Clade-Specific Quantitative Molecular Probes for Assessing Mercury Methylation in the Environment, *Appl. Environ. Microbiol.*, 2016, **82**, 6068–6078.
8 M. Podar, C. C. Gilmour, C. C. Brandt, A. Soren, S. D. Brown, B. R. Crable, A. V. Palumbo, A. C. Somenahally and D. A. Elias, Global prevalence and distribution of genes and microorganisms involved in mercury methylation, *Sci. Adv.*, 2015, **1**(9), DOI: 10.1126/sciadv.1500675.
9 C. C. Gilmour, M. Podar, A. L. Bullock, A. M. Graham, S. D. Brown, A. C. Somenahally, A. Johs, R. A. Hurt, K. L. Bailey and D. A. Elias, Mercury Methylation by Novel Microorganisms from New Environments, *Environ. Sci. Technol.*, 2013, **47**, 11810–11820.
10 L. Zeng, G. Luo, T. He, Y. Guo and X. Qian, Effects of sulfate-reducing bacteria on methylmercury at the sediment-water interface, *J. Environ. Sci.*, 2016, **46**, 214–219.
11 N. W. Johnson, C. P. J. Mitchell, D. R. Engstrom, L. T. Bailey, J. K. Coleman Wasik and M. E. Berndt, Methylmercury production in a chronically sulfate-impacted sub-boreal wetland, *Environ. Sci.: Processes Impacts*, 2016, **18**, 725–734.
12 A. Drott, L. Lambertsson, E. Björn and U. Skyllberg, Do Potential Methylation Rates Reflect Accumulated Methyl Mercury in Contaminated Sediments?, *Environ. Sci. Technol.*, 2008, **42**, 153–158.
13 H. Hsu-Kim, K. H. Kucharzyk, T. Zhang and M. A. Deshusses, Mechanisms Regulating Mercury Bioavailability for Methylating Microorganisms in the Aquatic Environment: A Critical Review, *Environ. Sci. Technol.*, 2013, **47**, 2441–2456.
14 G. Liu, Y. Cai and N. O'Driscoll, *Environmental Chemistry and Toxicology of Mercury*, Wiley, Hoboken, 1st edn, 2012.
15 A. G. Bravo, S. Bouchet, S. Guédron, D. Amouroux, J. Dominik and J. Zopfi, High methylmercury production under ferruginous conditions in sediments impacted by sewage treatment plant discharges, *Water Res.*, 2015, **80**, 245–255.
16 J. E. Gray and M. E. Hines, Biogeochemical mercury methylation influenced by reservoir eutrophication, Salmon Falls Creek Reservoir, Idaho, USA, *Chem. Geol.*, 2009, **258**, 157–167.
17 C. G. J. Hoggarth, B. D. Hall and C. P. J. Mitchell, Mercury methylation in high and low-sulphate impacted wetland ponds within the prairie pothole region of North America, *Environ. Pollut.*, 2015, **205**, 269–277.
18 R.-Q. Yu, J. R. Flanders, E. E. Mack, R. Turner, M. B. Mirza and T. Barkay, Contribution of Coexisting Sulfate and Iron Reducing Bacteria to Methylmercury Production in Freshwater River Sediments, *Environ. Sci. Technol.*, 2012, **46**, 2684–2691.
19 J. Stamenkovic, M. S. Gustin, M. C. Marvin-DiPasquale, B. A. Thomas and J. L. Agee, Distribution of total and methyl mercury in sediments along Steamboat Creek (Nevada, USA), *Sci. Total Environ.*, 2004, **322**, 167–177.
20 S. Haley, M. Klick, N. Szymoniak and A. Crow, Observing trends and assessing data for Arctic mining, *Polar Geogr.*, 2011, **34**, 37–61.
21 G. McMahon and F. Remy, *Large Mines and the Community: Socioeconomic and Environmental Effects in Latin America, Canada and Spain*, The World Bank, 2001.
22 V. N. de Jonge, M. Elliott and E. Orive, Causes, historical development, effects and future challenges of a common environmental problem: eutrophication, *Hydrobiologia*, 2002, **475**, 1–19.
23 M. J. Hird, Waste, Environmental Politics and Dis/Engaged Publics, *Theory Cult. Soc.*, 2017, **34**, 187–209.
24 INAC, *Giant Mine Remediation Project: Developer's Assessment Report*, 2010.
25 C. D. Anglin, *Gold in the Yellowknife greenstone belt, Northwest Territories: results of the EXTECH III multidisciplinary research project: collected papers and DVD of data reporting on results of the Yellowknife EXTECH III multidisciplinary research project*, Geological Association of Canada, Mineral Deposits Division, St. John's, Nfld, 2006.
26 J. Sandlos and A. Keeling, *Giant Mine: Historical Summary*, Memorial University, St. John's, N.L, 2015.
27 A. J. Houben, R. D'Onofrio, S. V. Kokelj and J. M. Blais, Factors Affecting Elevated Arsenic and Methyl Mercury Concentrations in Small Shield Lakes Surrounding Gold Mines near the Yellowknife, NT, (Canada) Region, *PLoS One*, 2016, **11**, e0150960.
28 M. J. Bromstad, L. A. Wrye and H. E. Jamieson, The characterization, mobility, and persistence of roaster-derived arsenic in soils at Giant Mine, NWT, *Appl. Geochem.*, 2017, **82**, 102–118.
29 H. E. Jamieson, The Legacy of Arsenic Contamination from Mining and Processing Refractory Gold Ore at Giant Mine, Yellowknife, Northwest Territories, Canada, *Rev. Mineral. Geochem.*, 2014, **79**, 533–551.
30 M. J. Bromstad, *The characterization, persistence, and bioaccessibility of roaster-derived arsenic in surface soils at Giant Mine*, NT Type: Master's thesis, Queen's University, Yellowknife, 2011.
31 S. M. Ullrich, T. W. Tanton and S. A. Abdrashitova, Mercury in the Aquatic Environment: A Review of Factors Affecting Methylation, *Crit. Rev. Environ. Sci. Technol.*, 2001, **31**, 241–293.
32 EPA, *Method 1631, Revision E: Mercury in Water by Oxidation, Purge and Trap, and Cold Vapor Atomic Fluorescence Spectrometry*, U.S. Environmental Protection Agency, Washington, DC, 2002.
33 Y. Cai, R. Jaffé, A. Alli and R. D. Jones, Determination of organomercury compounds in aqueous samples by capillary gas chromatography-atomic fluorescence spectrometry following solid-phase extraction, *Anal. Chim. Acta*, 1996, **334**, 251–259.

 This journal is © The Royal Society of Chemistry 2021

Published on 16 July 2021. Downloaded by University of Calgary on 6/22/2022 7:32:09 PM.

34 US EPA, *Method 200.8: Determination of Trace Elements in Waters and Wastes by Inductively Coupled Plasma-Mass Spectrometry*, U.S. EPA, Cincinnati, OH, 1994.
35 J. L. Weishaar, G. R. Aiken, B. A. Bergamaschi, M. S. Fram, R. Fujii and K. Mopper, Evaluation of Specific Ultraviolet Absorbance as an Indicator of the Chemical Composition and Reactivity of Dissolved Organic Carbon, *Environ. Sci. Technol.*, 2003, **37**, 4702–4708.
36 G. St-Jean, Automated quantitative and isotopic (13C) analysis of dissolved inorganic carbon and dissolved organic carbon in continuous-flow using a total organic carbon analyser, *Rapid Commun. Mass Spectrom.*, 2003, **17**, 419–428.
37 Y. Cai, R. Jaffé and R. Jones, Ethylmercury in the Soils and Sediments of the Florida Everglades, *Environ. Sci. Technol.*, 1997, **31**, 302–305.
38 B. L. Batista, J. L. Rodrigues, S. S. de Souza, V. C. O. Souza and F. Barbosa, Mercury speciation in seafood samples by LC–ICP-MS with a rapid ultrasound-assisted extraction procedure: Application to the determination of mercury in Brazilian seafood samples, *Food Chem.*, 2011, **126**, 2000–2004.
39 W. Zhu, Y. Song, G. A. Adediran, T. Jiang, A. T. Reis, E. Pereira, U. Skyllberg and E. Björn, Mercury transformations in resuspended contaminated sediment controlled by redox conditions, chemical speciation and sources of organic matter, *Geochim. Cosmochim. Acta*, 2018, **220**, 158–179.
40 I. Lehnherr, V. L. St. Louis, C. A. Emmerton, J. D. Barker and J. L. Kirk, Methylmercury Cycling in High Arctic Wetland Ponds: Sources and Sinks, *Environ. Sci. Technol.*, 2012, **46**, 10514–10522.
41 M.-L. Avramescu, E. Yumvihoze, H. Hintelmann, J. Ridal, D. Fortin and D. R. S. Lean, Biogeochemical factors influencing net mercury methylation in contaminated freshwater sediments from the St. Lawrence River in Cornwall, Ontario, Canada, *Sci. Total Environ.*, 2011, **409**, 968–978.
42 B. J. Callahan, P. J. McMurdie, M. J. Rosen, A. W. Han, A. J. A. Johnson and S. P. Holmes, DADA2: High-resolution sample inference from Illumina amplicon data, *Nat. Methods*, 2016, **13**, 581–583.
43 C. Quast, E. Pruesse, P. Yilmaz, J. Gerken, T. Schweer, P. Yarza, J. Peplies and F. O. Glöckner, The SILVA ribosomal RNA gene database project: improved data processing and web-based tools, *Nucleic Acids Res.*, 2013, **41**, D590–D596.
44 P. J. McMurdie and S. Holmes, Phyloseq: An R Package for Reproducible Interactive Analysis and Graphics of Microbiome Census Data, *PLoS One*, 2013, **8**, 1–11.
45 J. Oksanen, F. G. Blanchet, R. Kindt, P. Legendre, P. R. Minchin, R. B. O'Hara, G. L. Simpson, P. Solymos, M. H. H. Stevens, and H. Wagner, *Vegan: community ecology package. R package vegan, vers. 2.2-1*, 2015.
46 G. L. Simpson, *ggvegan; ggplot2-based plots for vegan*, 2019, https://github.com/gavinsimpson/ggvegan/.
47 W. N. Venables and B. D. Ripley, *Modern Applied Statistics with S*, Springer, New York, 4th edn, 2002.
48 A. Zeileis and T. Hothorn, *Diagnostic Checking In Regression Relationships*, R News.
49 J. Fox, S. Weisberg and J. Fox, *An R companion to applied regression*, SAGE Publications, Thousand Oaks, Calif, 2nd edn, 2011.
50 D. Borcard and P. Legendre, All-scale spatial analysis of ecological data by means of principal coordinates of neighbour matrices, *Ecol. Modell.*, 2002, **153**, 51–68.
51 P. Legendre, M. Fortin, D. Borcard and P. Peres-Neto, Should the Mantel test be used in spatial analysis?, *Methods Ecol. Evol.*, 2015, **6**, 1239–1247.
52 P. Legendre and M. J. Anderson, Distance-Based Redundancy Analysis: Testing Multispecies Responses in Multifactorial Ecological Experiments, *Ecol. Monogr.*, 1999, **69**, 1–24.
53 A. Canredon, P. Anschutz, D. Buquet, C. Charbonnier, D. Amouroux, E. Tessier, D. Poirier, S. Bujan, L. Devaux, B. Gouillieux, S. Gentès, A. Legeay, A. Feurtet-Mazel, S. Galaup and R. Maury-Brachet, Lake sediment mercury biogeochemistry controlled by sulphate input from drainage basin, *Appl. Geochem.*, 2019, **104**, 135–145.
54 C. C. Gilmour, G. S. Riedel, M. C. Ederington, J. T. Bell, G. A. Gill and M. C. Stordal, Methylmercury concentrations and production rates across a trophic gradient in the northern Everglades, *Biogeochemistry*, 1998, **40**, 327–345.
55 L. T. Bailey, C. P. J. Mitchell, D. R. Engstrom, M. E. Berndt, J. K. Coleman Wasik and N. W. Johnson, Influence of porewater sulfide on methylmercury production and partitioning in sulfate-impacted lake sediments, *Sci. Total Environ.*, 2017, **580**, 1197–1204.
56 T. Zhang, K. H. Kucharzyk, B. Kim, M. A. Deshusses and H. Hsu-Kim, Net Methylation of Mercury in Estuarine Sediment Microcosms Amended with Dissolved, Nanoparticulate, and Microparticulate Mercuric Sulfides, *Environ. Sci. Technol.*, 2014, **48**, 9133–9141.
57 C. S. Eckley and H. Hintelmann, Determination of mercury methylation potentials in the water column of lakes across Canada, *Sci. Total Environ.*, 2006, **368**, 111–125.
58 H. F. V. Braaten, H. A. de Wit, E. Fjeld, S. Rognerud, E. Lydersen and T. Larssen, Environmental factors influencing mercury speciation in Subarctic and Boreal lakes, *Sci. Total Environ.*, 2014, **476–477**, 336–345.
59 K. H. Kucharzyk, M. A. Deshusses, K. A. Porter and H. Hsu-Kim, Relative contributions of mercury bioavailability and microbial growth rate on net methylmercury production by anaerobic mixed cultures, *Environ. Sci.: Processes Impacts*, 2015, **17**, 1568–1577.
60 A. G. Bravo, S. Bouchet, J. Tolu, E. Björn, A. Mateos-Rivera and S. Bertilsson, Molecular composition of organic matter controls methylmercury formation in boreal lakes, *Nat. Commun.*, 2017, **8**, 14255.
61 H. Hintelmann, K. Keppel-Jones and R. D. Evans, Constants of mercury methylation and demethylation rates in sediments and comparison of tracer and ambient mercury availability, *Environ. Toxicol. Chem.*, 2000, **19**, 2204–2211.
62 I. Tjerngren, M. Meili, E. Björn and U. Skyllberg, Eight Boreal Wetlands as Sources and Sinks for Methyl Mercury in

Published on 16 July 2021. Downloaded by University of Calgary on 6/22/2022 7:32:09 PM.

Relation to Soil Acidity, C/N Ratio, and Small-Scale Flooding, *Environ. Sci. Technol.*, 2012, **46**, 8052–8060.

63 L. Windham-Myers, J. A. Fleck, J. T. Ackerman, M. Marvin-DiPasquale, C. A. Stricker, W. A. Heim, P. A. M. Bachand, C. A. Eagles-Smith, G. Gill, M. Stephenson and C. N. Alpers, Mercury cycling in agricultural and managed wetlands: a synthesis of methylmercury production, hydrologic export, and bioaccumulation from an integrated field study, *Sci. Total Environ.*, 2014, **484**, 221–231.

64 R. J. Strickman and C. P. J. Mitchell, Methylmercury production and accumulation in urban stormwater ponds and habitat wetlands, *Environ. Pollut.*, 2017, **221**, 326–334.

65 D. D. Bussan, R. F. Sessums and J. V. Cizdziel, Activated Carbon and Biochar Reduce Mercury Methylation Potentials in Aquatic Sediments, *Bull. Environ. Contam. Toxicol.*, 2016, **96**, 536–539.

66 R. Turpeinen, M. Pantsar-Kallio, M. Häggblom and T. Kairesalo, Influence of microbes on the mobilization, toxicity and biomethylation of arsenic in soil, *Sci. Total Environ.*, 1999, **236**, 173–180.

67 A. Mahamoud Ahmed, E. Lyautey, C. Bonnineau, A. Dabrin and S. Pesce, Environmental Concentrations of Copper, Alone or in Mixture With Arsenic, Can Impact River Sediment Microbial Community Structure and Functions, *Front. Microbiol.*, 2018, **9**, 1852.

68 S. A. Chiasson-Gould, J. M. Blais and A. J. Poulain, Dissolved Organic Matter Kinetically Controls Mercury Bioavailability to Bacteria, *Environ. Sci. Technol.*, 2014, **48**, 3153–3161.

69 E. B. Graham, J. E. Knelman, R. S. Gabor, S. Schooler, D. M. McKnight and D. R. Nemergut, Dissolved organic matter and inorganic mercury loadings favor novel methylators and fermentation metabolisms in oligotrophic sediments, *bioRxiv*, 2016, 072017.

70 T. D. French, A. J. Houben, J.-P. W. Desforges, L. E. Kimpe, S. V. Kokelj, A. J. Poulain, J. P. Smol, X. Wang and J. M. Blais, Dissolved Organic Carbon Thresholds Affect Mercury Bioaccumulation in Arctic Lakes, *Environ. Sci. Technol.*, 2014, **48**, 3162–3168.

71 C. A. Gerbig, C. S. Kim, J. P. Stegemeier, J. N. Ryan and G. R. Aiken, Formation of Nanocolloidal Metacinnabar in Mercury-DOM-Sulfide Systems, *Environ. Sci. Technol.*, 2011, **45**, 9180–9187.

72 A. Deonarine and H. Hsu-Kim, Precipitation of Mercuric Sulfide Nanoparticles in NOM-Containing Water: Implications for the Natural Environment, *Environ. Sci. Technol.*, 2009, **43**, 2368–2373.

73 A. M. Graham, G. R. Aiken and C. C. Gilmour, Dissolved organic matter enhances microbial mercury methylation under sulfidic conditions, *Environ. Sci. Technol.*, 2012, **46**, 2715–2723.

74 K. M. A. Paulson, C. J. Ptacek, D. W. Blowes, W. D. Gould, J. Ma, R. C. Landis and J. A. Dyer, Role of Organic Carbon Sources and Sulfate in Controlling Net Methylmercury Production in Riverbank Sediments of the South River, VA (USA), *Geomicrobiol. J.*, 2018, **35**, 1–14.

75 E. M. Smith and Y. T. Prairie, Bacterial metabolism and growth efficiency in lakes: The importance of phosphorus availability, *Limnol. Oceanogr.*, 2004, **49**, 137–147.

76 V. H. Smith, S. B. Joye and R. W. Howarth, Eutrophication of freshwater and marine ecosystems, *Limnol. Oceanogr.*, 2006, **51**, 351–355.

77 B. Meng, X. B. Feng, C. X. Chen, G. L. Qiu, J. Sommar, Y. N. Guo, P. Liang and Q. Wan, Influence of eutrophication on the distribution of total mercury and methylmercury in hydroelectric reservoirs, *J. Environ. Qual.*, 2010, **39**, 1624–1635.

78 M. Holmer and P. Storkholm, Sulphate reduction and sulphur cycling in lake sediments: a review, *Freshwater Biol.*, 2001, **46**, 431–451.

79 J. Zhao, X. Zhao, L. Chao, W. Zhang, T. You and J. Zhang, Diversity change of microbial communities responding to zinc and arsenic pollution in a river of northeastern China, *J. Zhejiang Univ., Sci., B*, 2014, **15**, 670–680.

80 Y. Li, J. Zhang, J. Zhang, W. Xu and Z. Mou, Microbial Community Structure in the Sediments and Its Relation to Environmental Factors in Eutrophicated Sancha Lake, *Int. J. Environ. Res. Public Health*, 2019, **16**, 1931.

81 Y. Zhao, M. Chen, J. Bai, X. Li, F. Zulfiqar and Q. Wang, Response of microbial community to petroleum stress and phosphate dosage in sediments of Jiaozhou Bay, China, *J. Ocean Univ. China*, 2014, **13**, 249–256.

82 J. Peuravuori and K. Pihlaja, in *Handbook of Water Analysis*, ed. L. M. L. Nollet and L. S. P. De Gelder, CRC Press, Boca Raton, 2nd edn, 2007, pp. 449–462.

83 K. K. Mueller, C. Fortin and P. G. C. Campbell, Spatial Variation in the Optical Properties of Dissolved Organic Matter (DOM) in Lakes on the Canadian Precambrian Shield and Links to Watershed Characteristics, *Aquat. Geochem.*, 2012, **18**, 21–44.

84 S. E. Johnston, R. G. Striegl, M. J. Bogard, M. M. Dornblaser, D. E. Butman, A. M. Kellerman, K. P. Wickland, D. C. Podgorski and R. G. M. Spencer, Hydrologic connectivity determines dissolved organic matter biogeochemistry in northern high-latitude lakes, *Limnol. Oceanogr.*, 2020, **65**, 1764–1780.

85 N. Udonna, P. Mason Robert, H. Zhang, S. Lin and T. Visscher Pieter, Effect of Inorganic and Organic Ligands on the Bioavailability of Methylmercury as Determined by Using a mer-lux Bioreporter, *Appl. Environ. Microbiol.*, 2012, **78**, 7276–7282.

86 M. Marvin-DiPasquale, J. Agee, C. McGowan, R. S. Oremland, M. Thomas, D. Krabbenhoft and C. C. Gilmour, Methyl-Mercury Degradation Pathways: A Comparison among Three Mercury-Impacted Ecosystems, *Environ. Sci. Technol.*, 2000, **34**, 4908–4916.

87 B. M. Miskimmin, J. W. M. Rudd and C. A. Kelly, Influence of Dissolved Organic Carbon, pH, and Microbial Respiration Rates on Mercury Methylation and Demethylation in Lake Water, *Can. J. Fish. Aquat. Sci.*, 1992, **49**, 17–22.

88 B. Ouddane, M. Monperrus, M. Kadlecova, M. Daye and D. Amouroux, Mercury methylation and demethylation in highly contaminated sediments from the Deûle River in Northern France using species-specific enriched stable isotopes, *Environ. Sci.: Processes Impacts*, 2015, **17**, 145–155.

 This journal is © The Royal Society of Chemistry 2021